

University of Groningen

## Validation of the Danckwerts-plot technique by simultaneous chemical absorption of CO<sub>2</sub> and physical desorption of O<sub>2</sub>

Cents, A. H. G.; De Bruijn, F. T.; Brilman, D. W. F.; Versteeg, G. F.

*Published in:*  
Chemical Engineering Science

*DOI:*  
[10.1016/j.ces.2005.05.021](https://doi.org/10.1016/j.ces.2005.05.021)

**IMPORTANT NOTE:** You are advised to consult the publisher's version (publisher's PDF) if you wish to cite from it. Please check the document version below.

*Document Version*  
Publisher's PDF, also known as Version of record

*Publication date:*  
2005

[Link to publication in University of Groningen/UMCG research database](#)

### *Citation for published version (APA):*

Cents, A. H. G., De Bruijn, F. T., Brilman, D. W. F., & Versteeg, G. F. (2005). Validation of the Danckwerts-plot technique by simultaneous chemical absorption of CO<sub>2</sub> and physical desorption of O<sub>2</sub>. *Chemical Engineering Science*, 60(21), 5809-5818. <https://doi.org/10.1016/j.ces.2005.05.021>

### **Copyright**

Other than for strictly personal use, it is not permitted to download or to forward/distribute the text or part of it without the consent of the author(s) and/or copyright holder(s), unless the work is under an open content license (like Creative Commons).

The publication may also be distributed here under the terms of Article 25fa of the Dutch Copyright Act, indicated by the "Taverne" license. More information can be found on the University of Groningen website: <https://www.rug.nl/library/open-access/self-archiving-pure/taverne-amendment>.

### **Take-down policy**

If you believe that this document breaches copyright please contact us providing details, and we will remove access to the work immediately and investigate your claim.

Downloaded from the University of Groningen/UMCG research database (Pure): <http://www.rug.nl/research/portal>. For technical reasons the number of authors shown on this cover page is limited to 10 maximum.

# Validation of the Danckwerts-plot technique by simultaneous chemical absorption of CO<sub>2</sub> and physical desorption of O<sub>2</sub>

A.H.G. Cents, F.T. de Bruijn, D.W.F. Brilman, G.F. Versteeg\*

*University of Twente, P.O. Box 217, 7500 AE Enschede, The Netherlands*

Received 7 July 2004; received in revised form 26 April 2005; accepted 5 May 2005

## Abstract

The Danckwerts-plot technique [Danckwerts et al., 1963. Chemical Engineering Science 18, 63–72] is used in chemical engineering to simultaneously obtain the mass transfer parameters,  $k_L$  and  $a$ , from mass transfer experiments. This method requires variation of the reaction kinetics by adding different amounts of catalyst. Although the method is known for several decades, it was never verified that the variation of the amount of catalyst does not affect the hydrodynamics of the system under investigation. To study this, absorption of CO<sub>2</sub> in a carbonate/bicarbonate buffer solution was performed simultaneously with desorption of oxygen from this solution, after verification that absorption and desorption are processes, taken place at identical rates, but in a different direction. It was shown that the addition of catalyst did not affect the desorption rate of oxygen. The obtained  $k_L a$  for oxygen was, however, 64% higher compared to the  $k_L a$  of carbon dioxide. This was probably due to a lower effective interfacial area, caused by the complete depletion of small bubbles containing CO<sub>2</sub>. Mass transfer experiments with oxygen, with a low gas phase conversion, are therefore to be preferred, as the measured mass transfer parameters are less affected by the gas phase RTD and the shape of the bubble size distribution.

© 2005 Elsevier Ltd. All rights reserved.

**Keywords:** Danckwerts-plot technique; Mass transfer; Interfacial area; Gas absorption

## 1. Introduction

The Danckwerts-plot technique was originally proposed by Danckwerts et al. (1963) and is a recognized method for simultaneous determination of the gas–liquid mass transfer coefficient ( $k_L$ ) and the specific interfacial area ( $a$ ). From the measurements of the gas absorption rate,  $R_A$  (mole/s), at different apparent first-order reaction rate constants the values of  $k_L$  and  $a$  can be determined simultaneously using the Danckwerts surface renewal model (Danckwerts, 1950) with a (pseudo)-first-order reaction:

$$\left( \frac{R_A}{m_{AC} V_L} \right)^2 = (k_L a)^2 + k_{1,app} D_A a^2. \quad (1)$$

When the left-hand side of Eq. (1) is plotted versus the apparent first-order rate constant times the diffusion coefficient of the gas into the liquid ( $k_{1,app} D_A$ ), the slope equals the squared specific gas liquid interfacial area ( $a^2$ ) and the intercept matches the square of the volumetric mass transfer coefficient ( $k_L a$ )<sup>2</sup>. The reactivity of the solution (the apparent first-order rate constant) is, therefore, changed by variation of the catalyst concentration in a catalyzed pseudo-first-order reaction or by changing the bulk concentration of the reactant that is used in excess in a pseudo-first-order reaction. A reaction system that is very suitable for this technique is the absorption of CO<sub>2</sub> in carbonate/bicarbonate buffer solutions. The dissolved CO<sub>2</sub> can react with water as well as with hydroxyl ions, which are formed from the equilibrium between carbonate and bicarbonate ions. The overall reaction that occurs is



\* Corresponding author. Tel.: +31 53 489 3327; fax: +31 53 489 4774.

E-mail address: [g.f.versteeg@utwente.nl](mailto:g.f.versteeg@utwente.nl) (G.F. Versteeg).

The reaction of CO<sub>2</sub> and water can be catalyzed by a number of compounds, e.g. hypochlorite, arsenite, carbonic anhydrase and different sugars. The apparent first-order rate constant for this system is given by

$$k_{1,\text{app}} = k_{\text{H}_2\text{O}} + k_{\text{OH}^-}[\text{OH}^-] + k_c[\text{cat}]. \quad (3)$$

From this equation it must be concluded that the apparent first-order reaction system is in fact a much more complex system. For a more detailed description of this reaction system the reader is referred to Cents (2003). For a convenient and accurate description of the absorption process it is important that the reaction can be assumed to be pseudo-first-order in the hydroxyl and/or catalyst concentration. To consider the reaction to be pseudo-first order, it is important that the concentrations of all the ionic species (CO<sub>3</sub><sup>2-</sup>, HCO<sub>3</sub><sup>-</sup>, H<sup>+</sup> and OH<sup>-</sup>) up to the interface are uniform and identical to the bulk concentrations, i.e. no depletion of ionic species within the mass transfer zone. The criterion that determines whether the concentrations of all ions are uniform, throughout the mass transfer zone, was derived by Danckwerts and Sharma (1966):

$$m[\text{CO}_2] \left( \frac{1}{[\text{CO}_3^{2-}]} + \frac{2}{[\text{HCO}_3^-]} \right) \times \left( \sqrt{1 + \frac{D_{\text{CO}_2} k_{1,\text{app}}}{k_L^2}} - 1 \right) \ll 1. \quad (4)$$

In this equation full dissociation of the catalyst ion is assumed, which is generally the case when sodium hypochlorite is used as a catalyst (Danckwerts et al., 1963). The validity of this criterion is discussed more thoroughly by Cents et al. (in press).

The Danckwerts-plot technique has been applied for a long time in literature (Richards et al., 1964; Mehta and Sharma, 1971; Kon and Sandall, 1978; Alper et al., 1980; Benadda et al., 1994) and usually a straightline is obtained, when plotting Eq. (1), which suggests that the method is valid for the systems used. In order to validate the Danckwerts method, Kon and Sandall (1978) and Alper et al. (1980) used gas absorption in a liquid with a flat interface to test the technique by comparison of the known geometric gas–liquid interfacial area with the area as determined by the Danckwerts-plot. The first authors found the interfacial area determined with the Danckwerts plot to be considerably less than the actual geometric interfacial area, although they obtained straightlines using Eq. (1). Alper et al. (1980), however, performed similar experiments and found straightlines, but only upto  $k_{1,\text{app}} = 6 \text{ s}^{-1}$ . Beyond this value the slope of the line decreased, due to non-uniform ion concentrations (the criterion in Eq. (4) was no longer satisfied), at least according to the authors. The slope of the plot up to  $k_{1,\text{app}} = 6 \text{ s}^{-1}$  was indeed equal to the square of the geometric gas–liquid interfacial area. Alper et al. (1980) also discussed in detail the results of Kon and Sandall (1978) critically and

concluded that the results of the latter authors were not reliable because the criterion in Eq. (4) was not fulfilled.

This example shows that obtaining a straightline from the Danckwerts plot does not automatically imply that all requirements for successful application of the technique are fulfilled. Alper et al. (1980) have tested the method only up to catalyst concentrations of 0.02 M. That means that no experimental evidence is provided that the addition of larger amounts of catalyst (which is necessary in systems with a higher mass transfer coefficient), does not influence the physical properties that may affect the hydrodynamics of the system, which could lead to erroneous determinations of the mass transfer parameters. It is not possible to test this at concentration above 0.02 M using gas absorption in a stirred cell with a flat interface, because then the criterion in Eq. (4) can never be fulfilled due to the relatively low value of the mass transfer coefficient.

To study the influence of the catalyst on hydrodynamics, the mass transfer rate of a non-reactive gas can be determined simultaneously with the chemical absorption of a reactive gas. When the gas–liquid mass transfer rate of the non-reactive gas is not influenced by the addition of the catalyst, the assumption that the catalyst does not change the hydrodynamics of the system is very likely to hold. The main objective of the present study is therefore to validate the results obtained by Cents et al. (2001) by showing that the hydrodynamics of the reaction system used were not affected, by adding different amounts of catalyst, when the Danckwerts-plot technique is applied.

## 2. Experimental

To study the influence of the catalyst on hydrodynamics, the mass transfer rate of a non-reactive gas can be determined simultaneously with the chemical absorption of the reactive gas. The reactive system used in this work is the chemical absorption of CO<sub>2</sub> in potassium carbonate/bicarbonate solutions in which the reactivity was varied using different concentrations of sodium hypochlorite as a catalyst.



The simultaneously occurring physical mass transfer experiment for a non-reacting gas phase component should now be selected and designed. In order to arrive at an optimum system for this purpose, a more detailed analysis is presented here.

### 2.1. Design criteria for physical mass transfer experiments

In order to obtain an accurate determination of  $k_L a$  for the non-reactive gas, design criteria for physical mass transfer experiments are derived. In case of a chemical system the liquid can often be operated batchwise. This method of operation can also be used in case of physical mass transfer

measurements (dynamic methods, e.g. Linek et al. (1987)), but a continuous operation of the liquid phase is more accurate, and will therefore be used in this work. Two choices must be made to arrive at the most accurate method to determine the mass transfer rate: firstly, the outlet concentration can be measured in the gas phase or in the liquid phase and, secondly, the direction of mass transfer of the gas phase component (absorption or desorption) is a degree of freedom, under the assumption that these are mirror image processes. For the first selection a criterion is derived based upon the relative change in outlet concentration with a variation in  $k_L a$ . If it is assumed that the accuracy of the measurement in the liquid phase is equal to the measurement in the gas phase, the variation of the outlet concentration with  $k_L a$  determines the overall accuracy of the measurement. In a system with a continuous and well-mixed liquid phase and a continuous well-mixed gas phase the steady-state mass balances for the component to be transferred in the gas and the liquid phases, respectively, are:

$$0 = \frac{\Phi_G}{V_L}(c_{G,0} - c_G) - k_L a(m c_G - c_L), \quad (6)$$

$$0 = \frac{\Phi_L}{V_L}(c_{L,0} - c_L) + k_L a(m c_G - c_L). \quad (7)$$

From these two balances, the volumetric mass transfer coefficient can be determined by making use of the steady-state concentration in the gas- or in the liquid phase outlet stream, which will be measured experimentally.

The  $k_L a$  based on gas phase analysis is then given by

$$k_{L a \text{ GAS}} = \frac{c_{G,0} - c_G}{(V_L/\Phi_G)(m c_G - c_{L,0}) + (V_L/\Phi_L)(c_G - c_{G,0})} \quad (8)$$

and the  $k_L a$  based on liquid phase analysis equals:

$$k_{L a \text{ LIQ}} = \frac{c_L - c_{L,0}}{m(V_L/\Phi_G)(c_{L,0} - c_L) + (V_L/\Phi_L)(m c_{G,0} - c_L)}. \quad (9)$$

For both these cases it is possible to calculate the change in the outlet concentration in the steady state with a small variation in  $k_L a$  (thus  $dc/d(k_L a)$ ). This ratio is shown in Figs. 1A and B in case of desorption for two different values of the distribution coefficient,  $m$  ( $m = 0.9$  resembles carbon dioxide and  $m = 0.032$  resembles oxygen).

A large value for  $dc/d(k_L a)$  means that a small variation in  $k_L a$  causes a relatively large change in the experimentally measured outlet concentration, which improves the accuracy of the measurement. It is clear from Fig. 1 that in case of oxygen desorption, measurement of the concentration in the liquid phase is more accurate and in case of desorption of  $\text{CO}_2$  the concentration is preferably determined in the gas phase.

In general, a relation can be derived from the ratio of this parameter using gas phase analysis and when using liquid

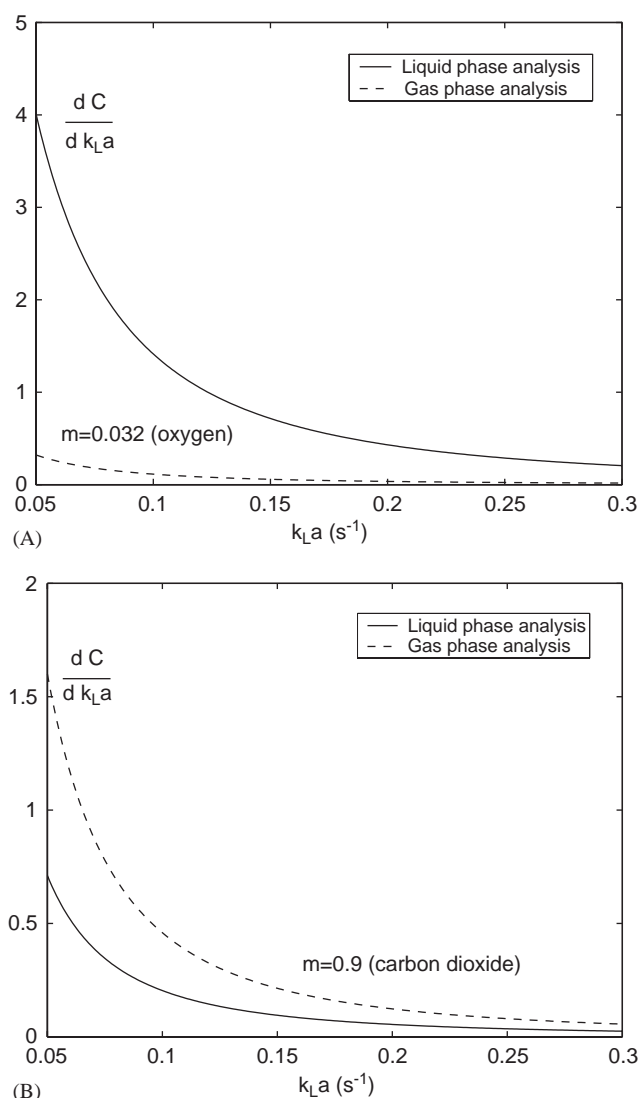


Fig. 1. The variation of the normalized concentration ( $C = c/c_0$ ) with  $k_L a$  as a function of  $k_L a$ . (A)  $m = 0.032$ , (B)  $m = 0.9$ .  $V_L/\Phi_G = 100$  s and  $V_L/\Phi_L = 40$  s in both cases.

phase analysis. This ratio can be determined, and is identical, for both absorption ( $c_{L,i} = 0$ ) and desorption ( $c_{G,i} = 0$ ) experiments and equals:

$$\frac{dc_G/d(k_{L a \text{ GAS}})}{dc_L/d(k_{L a \text{ LIQ}})} = \frac{m\Phi_L}{\Phi_G}. \quad (10)$$

Using this relation it can be seen that for  $m\Phi_L > \Phi_G$  concentration measurement in the gas phase is favourable and vice versa.

The second selection (absorption or desorption) depends upon the first one, because desorption is favoured in case of liquid concentration measurement and absorption in case of gas phase measurement. This can be shown from a sensitivity analysis for the effects of small disturbances in temperature and pressure on determination of the volumetric mass transfer coefficient (for details, see Cents, 2003). In general,

Table 1  
Design criteria for physical mass transfer experiments

Favourable	Gas phase measurement	Liquid phase measurement
Absorption	$m\Phi_L > \Phi_G$	Never
Desorption	Never	$m\Phi_L < \Phi_G$

it is favourable when the dimensionless concentration ratio in the reactor ( $c/c_0$ ) can be used, which means that absorption should be used for gas phase analysis and desorption for liquid phase experiments. The design criteria for physical mass transfer experiments are summarized in Table 1.

In the present study oxygen was selected as the non-reactive gas and by using the above criteria it was calculated that the influence of the addition of catalyst in the chemical absorption of CO<sub>2</sub> can best be studied with the desorption of O<sub>2</sub> using liquid phase analysis. An important prerequisite is that absorption and desorption are mirror-image processes. This aspect will be studied first (and the validity of this assumption will be demonstrated) by comparing absorption and desorption rates of oxygen in water.

## 2.2. Physical parameters

The estimation of the physical parameters that are required for simultaneous determination of  $k_L$  and  $a$  using the Danckwerts-plot at 21 °C are presented elsewhere (Cents et al., 2001). All experiments are conducted at a total pressure close to and just above atmospheric pressure. The mole

fraction of oxygen in water at 1 atm partial pressure of oxygen is taken from IUPAC Solubility Data Series (Lorimer, 1979). The distribution coefficient of oxygen  $m_{O_2}$  in water was derived from the mole fraction and was calculated to be 0.0326 at 21 °C. The salting out effect that decreases the oxygen solubility was estimated using the Sechenov equation and the parameters were taken from Weisenberger and Schumpe (1996). The oxygen distribution coefficient in the 0.6/0.6 M potassium carbonate/potassium bicarbonate buffer was determined to be 0.0160 at 21 °C.

## 2.3. Experimental set-up

The absorption and desorption experiments were performed in a set-up which consisted of a liquid storage vessel, in which the aqueous solution was saturated with the gas, a stirred reactor with a maximum working volume of 3.5 l and an analytical section. A schematical representation of the set-up is presented in Fig. 2. The liquid is pumped into the reactor from the storage vessel and the oxygen content of the liquid leaving the reactor can be measured using a dissolved oxygen meter. Gas entering the reactor is brought to the desired composition using mass flow controllers and the outlet carbon dioxide gas concentration can be determined using an infrared gas-analyzer (UNOR, Maihak). The gas phase oxygen concentration was determined by a paramagnetic oxygen analyzer. Before the gas is sent to the analyzers it was cooled to −6 °C to remove water. In the reactor a six-bladed Rushton turbine and four baffles ensure adequate mixing and the power input can be set to any desired level. All dimensions are given in Table 2. In all experiments a volume fraction of 1.7% CO<sub>2</sub> was used and

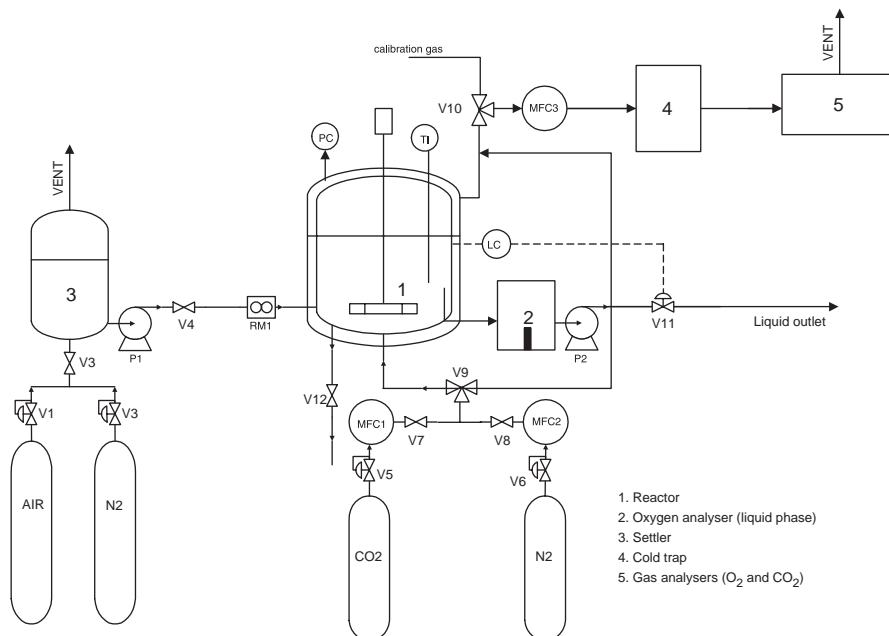


Fig. 2. Experimental set-up.



Table 2  
Standard reactor dimensions

Parameter	Symbol	Value	Dimension	Remarks
Tank diameter	$T$	0.149	m	
Impeller diameter	$D$	0.049	m	
Liquid volume	$V$	2.53	dm <sup>3</sup>	
Impeller blade width	$W$	9.3	mm	
Impeller blade length	$L_B$	12.3	mm	
Baffle width	$B$	15.0	mm	
Impeller height above bottom	$H_I$	0.049	m	
Impeller power number	$N_P$	5.8	—	
Diameter of the sparger	$d_s$	3	mm	1 hole below the impeller
Height of the sparger	$h_s$	20	mm	Above the bottom

oxygen was introduced as air (20.9%). The total pressure was just above atmospheric pressure (1.05–1.2 bar).

### 3. Results and discussion

#### 3.1. Physical mass transfer experiments

To test the experimental technique a mass balance check was performed using gas- and liquid phase oxygen analysis in both absorption and desorption experiments. An example of an experiment is presented in Fig. 3. The maximum error in the mass balance experiments was 2% of the total moles of oxygen, which is sufficiently accurate.

To validate that absorption and desorption are exactly identical processes, but in a different direction, absorption and desorption experiments of oxygen in water were compared at different liquid hold-up volumes (1.5–3.5 l), different gas flow rates (0.27–11.8 l/min) and different gassed power inputs (1–7 × 10<sup>3</sup> W/m<sup>3</sup>). The results of these experiments are presented in Table 3.

From Table 3 it can be seen that absorption and desorption are mirror image processes for all the conditions used in this research. As expected from the design criteria for physical mass transfer experiments desorption experiments are somewhat more accurate than absorption experiments.

The determined  $k_L a$  values for both absorption and desorption, respectively, can be compared with the results from the work of Linek et al. (1987), who measured oxygen mass transfer coefficients using different methods and combined these data with experimental results from literature to obtain:

$$k_L a = 4.95 \times 10^{-3} \left( \frac{P_g}{V_L} \right)^{0.593} u_G^{0.4}. \quad (11)$$

In this correlation,  $u_G$  is the superficial gas velocity and  $P_g/V_L$  is the gassed power input per unit of volume. The ungassed power input ( $P$ ) is given by

$$P = N_P \rho N^3 D^5. \quad (12)$$

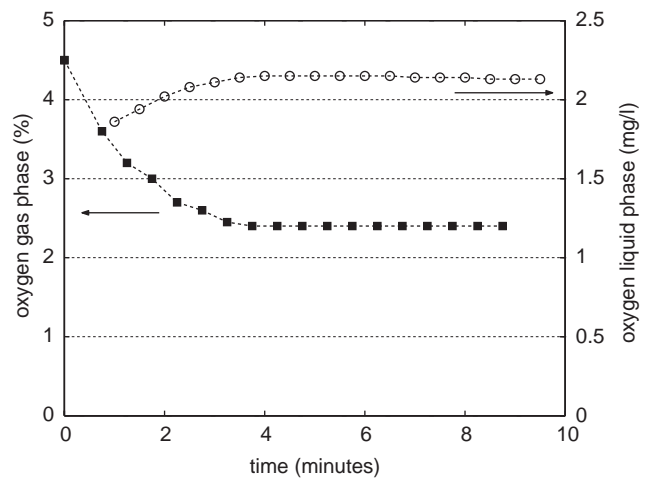


Fig. 3. Mass balance experiment ( $V_L = 3.49 \times 10^{-3}$  m<sup>3</sup>,  $\Phi_L = 2.15 \times 10^{-5}$  m<sup>3</sup>/s,  $\Phi_G = 4.48 \times 10^{-6}$  m<sup>3</sup>/s,  $T = 21$  °C,  $p = 1.05$  bar).

Hughmark (1980) correlated an extensive amount of data on the influence of the sparged gas on the power input and found the following relation:

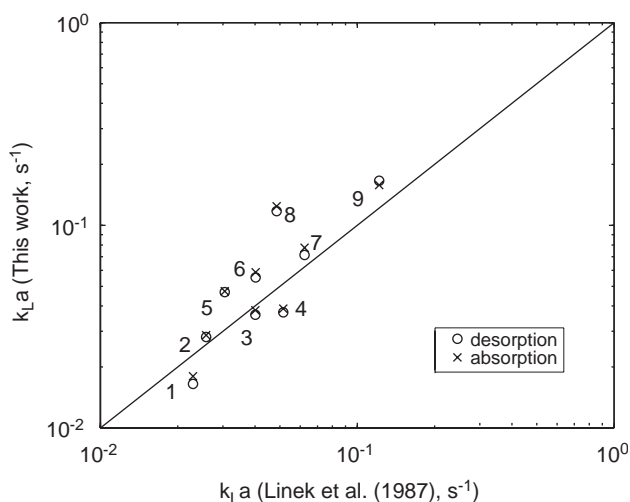
$$\frac{P_g}{P} = 0.10 \left( \frac{\Phi_G}{N V_L} \right)^{-1/4} \left( \frac{N^2 D^4}{W_g V_L^{2/3}} \right)^{-1/5}. \quad (13)$$

A comparison between the data obtained in this work and the correlation of Linek et al. (1987) is shown in Fig. 4 in a parity plot. From this figure it can be concluded that the range of the obtained mass transfer coefficients is in agreement with Eq. (11), but the deviation from the correlation is rather large (an average relative deviation of 32%). The root cause of this deviation can probably be found in the non-standard tank dimensions and the wide range of conditions used in the experiments. The standard dimensions of the experimental set-up included that  $V_L = 2.53$  dm<sup>3</sup>, which means that the clear liquid height is equal to the tank diameter ( $H_L = T$ ) and the distance from the bottom to the impeller is one-third of the clear liquid height ( $H_I = 1/3 H_L$ ). In the experiments with standard dimensions (2, 6, 7 and 9) the trend of Eq. (11) is well followed, but a somewhat higher  $k_L a$  is

Table 3

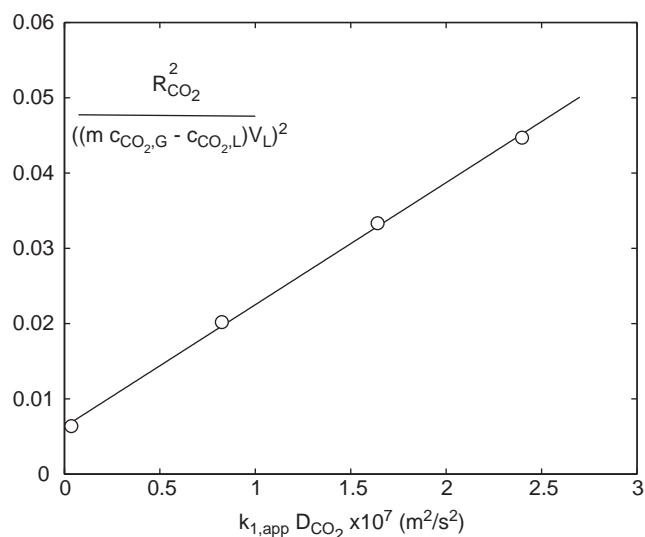
Comparison of absorption and desorption rates of oxygen in water

Exp.	Volume liquid, $V_L$ (dm <sup>3</sup> )	Gas flow rate, $\Phi_{G,0}$ (dm <sup>3</sup> /min)	Liquid flow rate, $\Phi_L$ (dm <sup>3</sup> /min)	$N$ (rpm)	# of des.	# of abs.	$k_L a$ desorption (s <sup>-1</sup> )	$k_L a$ absorption (s <sup>-1</sup> )	Relative deviation (%)
1	3.49	0.628	3.1	1000	2	3	0.017±2%	0.018±4%	– 6
2	2.53	0.628	3.1	1000	5	8	0.028±3%	0.029±10%	– 2
3	3.38	3.73	1.26	1060	1	1	0.036	0.038	– 5
4	3.49	0.27	1.26	1830	3	2	0.037±13%	0.039±1%	– 4
5	1.69	0.635	3.1	1010	5	12	0.046±5%	0.047±8%	– 2
6	2.53	0.628	3.1	1300	5	4	0.056±4%	0.059±3%	– 5
7	2.53	11.7	1.25	1090	7	5	0.071±6%	0.078±2%	– 8
8	1.69	0.635	3.1	1330	6	10	0.119±3%	0.124±9%	– 4
9	2.53	11.7	1.23	1620	2	2	0.166±5%	0.158±12%	+ 6

Fig. 4. Comparison of absorption and desorption experiments with the correlation of Linek et al. (1987).  $T = 21^\circ\text{C}$ .

obtained in this work. The main deviation from the correlation is observed for the experiments with non-standard tank dimensions:  $V_L = 3.49\text{ dm}^3$  ( $H_L/T = 1.38$ , exp:1,4), and when  $V_L = 1.69\text{ dm}^3$  ( $H_L/T = 0.67$ , exp:5,8).

These results suggest that the effect of the liquid volume is not taken into account correctly. This phenomenon was also observed by Schlüter and Deckwer (1992) who suggested that instead of the superficial gas velocity ( $u_G$ ) the space velocity of the gas ( $\phi_G = \Phi_G/V_L$ ) should be used in the data correlation. Doing so, the average relative deviation decreased by more than 50%. The best values for the coefficients were obtained by a least-squares regression analysis of the experimental values, which resulted in:  $k_L a = 1.5 \times 10^{-3} (P_g/V)^{0.67} \phi_G^{0.4}$ . The exponent for the power input per unit volume (0.67) obtained in this correlation is in reasonable agreement with the work of Linek et al. (1987), 0.593 and with the work of Schlüter and Deckwer (1992), 0.62. The influence of the space velocity on the volumetric mass transfer coefficient is larger in this work (exponent of 0.4)

Fig. 5. Danckwerts plot with batchwise operation of the liquid phase,  $T = 21^\circ\text{C}$ .

compared to the correlation of Schlüter and Deckwer (1992) (0.23). The effect of the gas flow rate, which is present in  $u_G$  as well as in  $\phi_G$ , is, however, exactly equal to the effect in the work of Linek et al. (1987).

### 3.2. Chemical absorption of $\text{CO}_2$ compared to physical desorption of $\text{O}_2$

In the first set of experiments for the Danckwerts-plot, the liquid phase was operated batchwise. As a buffer solution 0.5/0.5 M potassium carbonate/potassium bicarbonate was chosen. Using different molarities of sodium hypochlorite the Danckwerts-plot as given in Fig. 5 was determined. The experimental conditions are given in Table 4.

From the slope and the intercept of this graph the following results are obtained, when both phases are assumed to be ideally mixed:  $k_L = 2.0 \times 10^{-4}\text{ m/s}$ ,  $a = 403\text{ m}^2/\text{m}^3$ ,  $k_L a = 0.079\text{ s}^{-1}$ . Cents (2003) has shown that the absolute values of the individual mass transfer parameters,  $k_L$  and

Table 4

Experimental conditions used in the chemical absorption/physical desorption experiments in a 0.6/0.6 M potassium carbonate/bicarbonate buffer solution

	Continuous	Batch
Gas flow rate, $\Phi_G$ (m <sup>3</sup> /s <sup>1</sup> )	$1.98 \times 10^{-4}$	$1.95 \times 10^{-4}$
Liquid flow rate, $\Phi_L$ (m <sup>3</sup> /s <sup>1</sup> )	$5.17 \times 10^{-5}$	—
Liquid volume reactor, $V_L$ (m <sup>3</sup> )	$2.53 \times 10^{-3}$	$2.53 \times 10^{-3}$
Impeller speed, $N$ , (rps)	18.3	18.3
Temperature, $T$ (°C)	21.0	21.0
Reactor pressure, $p$ (bar)	1.18	1.18
Catalyst concentration, $c_{\text{cat}}$ (mol/m <sup>3</sup> )	0–178	0–92

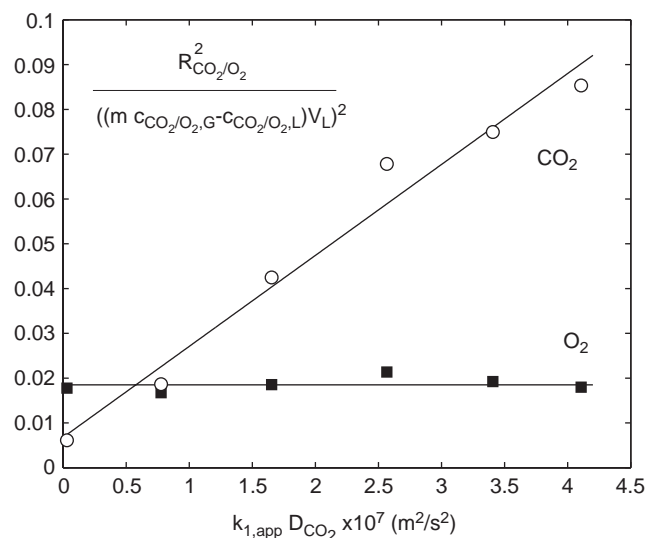


Fig. 6. Validation of the Danckwerts-plot technique by comparison of the absorption rate of carbon dioxide and the desorption rate of oxygen at different catalyst (NaOCl) concentrations.  $T = 21$  °C.

$a$ , depend on the assumed gas phase mixing pattern. The Danckwerts-plot technique can, however, be used to measure relative differences in the mass transfer parameters. In addition, the absolute value for the product of  $k_L$  and  $a$ ,  $k_L a$  is always obtained accurately.

The measurements for the validation of the Danckwerts-plot technique are represented in Fig. 6 showing the absorption rate of carbon dioxide and the desorption rate of oxygen for increasing catalyst concentration. The experimental conditions are given in Table 4.

As is shown in Fig. 6, the rate of desorption of oxygen from the liquid phase is not influenced by the addition of catalyst up to 178 mol/m<sup>3</sup>. Deviations from the average are most likely due to experimental errors. This is supported by the fact that the deviations occur simultaneously for carbon dioxide and for oxygen and in the same direction. The chemical absorption measurements of carbon dioxide are somewhat more inaccurate when the reactor is operated continuously than when the liquid phase is operated batchwise (compare Figs. 5 and 6), probably due to a more difficult

operation of the set-up. Also the obtained mass transfer parameters deviate (max. 20%) from the batchwise operation. The results for carbon dioxide are (under the assumption of an ideally mixed gas and liquid phase):

$$k_L = 1.8 \times 10^{-4} \text{ m/s}, a = 451 \text{ m}^2/\text{m}^3, k_L a = 0.083 \text{ s}^{-1}.$$

The results of the present study show very clearly that the addition of catalyst does not influence the physical desorption of oxygen and that the application of the Danckwerts-plot is allowed over a large concentration range.

The absolute value of the volumetric mass transfer coefficient of oxygen is, however, not completely in line with the  $k_L a$  of carbon dioxide. The average  $k_L a$  for oxygen is found to be  $0.136 \text{ s}^{-1} \pm 5\%$ , which is 64% higher than the  $k_L a$  for carbon dioxide under similar conditions. This cannot be explained with the existing theories for mass transfer, from which a relationship of the following form would be expected:

$$(k_L a)_{\text{O}_2} = (k_L a)_{\text{CO}_2} \left( \frac{D_{\text{O}_2}}{D_{\text{CO}_2}} \right)^n, \quad (14)$$

where  $n$  is typically between 0.5 and 1. The observed large difference in volumetric mass transfer cannot be explained by the difference in the diffusion coefficients, because the diffusion coefficient of oxygen is approximately only 16% higher than the diffusion coefficient of carbon dioxide (assuming that the ratio in the buffer solution is equal to the ratio in water, which was taken from the work of Díaz et al. (1987)). Furthermore, the observed difference in  $k_L a$  cannot be explained by the assumed gas-phase residence time distribution (CISTR), as an analysis. Cents et al. (2003) has shown that this difference increases with decreasing gas phase mixing.

A possible explanation for the observed discrepancy may be attributed to the difference in solubility in water of oxygen and carbon dioxide. The solubility of carbon dioxide is approximately 25–30 times higher when compared to the oxygen solubility. This can cause differences in the effective gas–liquid interfacial area when the bubble size is non-uniform and consists of a certain size distribution. Small bubbles containing carbon dioxide deplete much faster from the gas to be absorbed and therefore stop taking part in the mass transfer process at an earlier stage compared to bubbles containing oxygen. These effects were also recognized and analysed by Schumpe and Deckwer (1980), who compared interfacial area data in bubble columns reported by different authors that either made use of CO<sub>2</sub> absorption in alkali or used O<sub>2</sub> absorption in sulphite solutions. Under (approximately) identical conditions oxygen absorption in sulphite solutions yields interfacial areas that are 50–500% higher compared to absorption of carbon dioxide in alkali solutions. An attempt was made to model these effects by taking the size distributions and the corresponding bubble rise velocities into account. To be able to explain the observed large differences in the interfacial area very broad size distributions should be assumed, containing a relatively



large fraction of small bubbles, with a long residence time in solution.

Another explanation for this phenomenon can be a smaller mass transfer coefficient,  $k_L$ , in case of carbon dioxide. Hallensleben (1980) measured lower values for the  $k_L$  of carbon dioxide compared to oxygen in water and showed that the values were both dependent on the inlet concentrations and on the direction of mass transfer. Hallensleben stated that the lower  $k_L$  might be due to a resistance in the gas phase, although this was not expected at these low  $k_L$  values ( $2\text{--}3 \times 10^{-4}$  m/s). To be able to explain the observed phenomenon a  $k_G$  value of  $1 \times 10^{-3}$  m/s should be assumed which is an order of magnitude lower than expected (by taking for instance the correlations from Carberry and Varma (1987)). Furthermore, in the work by Hallensleben the  $k_L$  was determined by indirect measurement of the  $k_L a$  and the interfacial area that was determined by photography, which means that these results only indicate that there might be a difference between absorption of oxygen and carbon dioxide, but it is not clear whether this effect is due to a different effective interfacial area or due to a different mass transfer coefficient. Measurement of the  $k_L$  for a single rising bubble did not show a difference between  $\text{O}_2$  and  $\text{CO}_2$  that could not be explained by differences in the diffusion coefficients as was shown by Hallensleben (1980).

To gain understanding about the nature of the measured differences, three additional types of experiments were conducted in the present study:

- (1) Absorption of pure  $\text{CO}_2$  (no gas phase resistance) in non-coalescing water–butyraldehyde solutions was performed in a 600 ml vessel, equipped with a gas-inducing impeller, in order to determine the effect of the gas phase resistance. The  $k_L a$  obtained with pure  $\text{H}_2$ ,  $\text{CO}$  and propylene was on average 75% higher compared to  $\text{CO}_2$  (after correction for the diffusion coefficients, see Fig. 7), which indicates that (at least in this case) the gas phase resistance is not likely to be responsible for the obtained lower volumetric mass transfer coefficients. The difference in these experiments is most likely caused by the higher shrinking rate of gas bubbles containing  $\text{CO}_2$  compared to the other gasses, which causes a lower interfacial area.
- (2) The interfacial area measured with the Danckwerts-plot technique was compared with the area determined using ultrasonic spectroscopy (Cents et al., 2004). Although the absolute value of the interfacial area as determined by the Danckwerts-plot depend on the assumed residence time distribution (RTD) of the gas phase, it was shown that even at the RTD assumption which yields the largest interfacial area (CISTR), the value of the interfacial area measured by the ultrasonic technique is on average 70% higher. These measurements were performed in a 601 stirred vessel with a Rushton turbine, and the results at two different stirring speeds are presented in Table 5. The obtained difference is probably higher, as

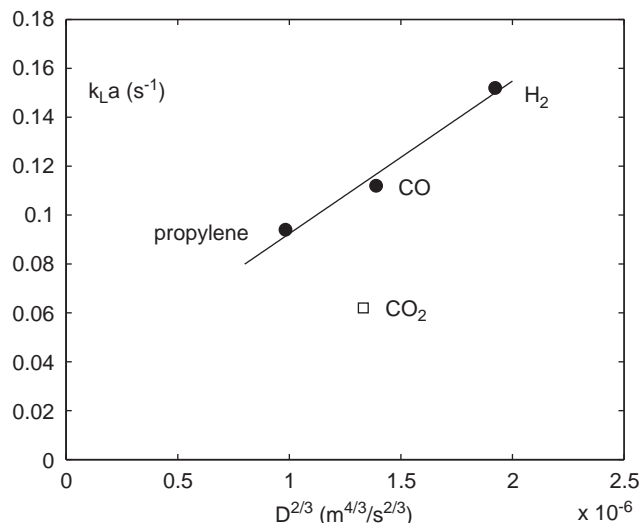


Fig. 7. Volumetric mass transfer coefficients of pure gasses.

the measured RTD curves in the non-coalescing buffer system show increasing plug flow behaviour with increasing stirrer speed (Cents, 2003). These results indicate that the (effective) interfacial area as measured by the  $\text{CO}_2$  absorption using the Danckwerts-plot technique is smaller than the actual interfacial area.

- (3) An indication of the width and shape of the bubble size distribution was obtained using the ultrasonic technique by measurement of the profiles of the ultrasonic velocity and attenuation coefficient versus frequency. A good fit between the measured profiles and the model could only be obtained with a distribution that contained a large fraction of small ( $< 100 \mu\text{m}$ ) bubbles (either in a very broad log-normal distribution or in a bimodal distribution). The presence of large fractions of small bubbles was also measured by Machon et al. (1997), who used a microscope/video technique to study bubble size distributions in coalescing and non-coalescing systems. The bubble size distributions that were obtained, were used in a mass transfer modelling study, details of which can be found elsewhere (Cents, 2003). In Fig. 8 the conversion per bubble class is shown for physical oxygen absorption in the 0.6/0.6 M buffer solution ( $m = 0.016$ ) and for chemical absorption of carbon dioxide in the buffer solution ( $m = 0.50$ ). In case of  $\text{CO}_2$  absorption bubbles of  $440 \mu\text{m}$  are already completely (99%) depleted from the gas, while in case of oxygen absorption this is only the case for bubbles up to  $100 \mu\text{m}$  in diameter. (These results differ slightly at different size distributions.) In case of a broad bubble size distribution containing small bubbles, large differences in the measured mass transfer rate of oxygen and carbon dioxide can therefore occur.

To study the effect of the ratio of the measured interfacial area and the geometrical interfacial area, two size distributions were investigated; the size distribu-

Table 5

Comparison of the interfacial area as determined with the ultrasonic method and with the Danckwerts-plot technique (assuming ideally mixed gas phase)

	$k_L a$ ( $s^{-1}$ )	$a$ ( $m^2/m^3$ )	$k_L$ (m/s)	$\varepsilon$ (%)	$d_{32}$ (mm)
430 rpm					
Physical (ultrasound)	—	784	—	11.8	0.90
Chemical (Danckwerts-plot)	0.055	433	$1.3 \times 10^{-4}$	—	—
550 rpm					
Physical (ultrasound)	—	1084	—	13.3	0.74
Chemical (Danckwerts-plot)	0.102	667	$1.5 \times 10^{-4}$	—	—

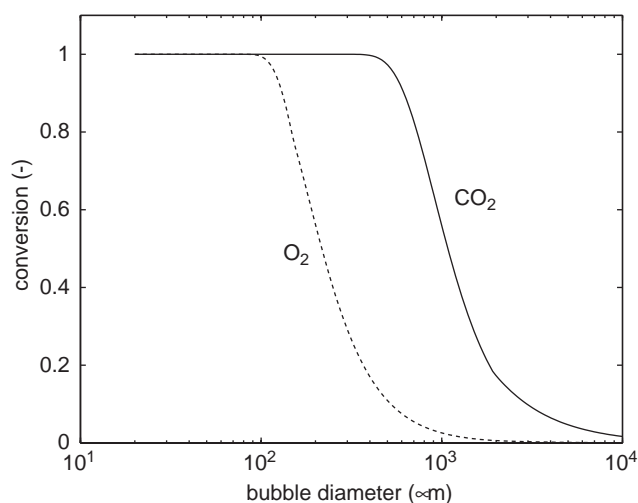
Fig. 8. Depletion from the absorbed gas of different bubble sizes. (Log-normal distribution ( $\mu = 0.36$  mm,  $\sigma = 0.25$  mm)).

Table 6

Ratio of interfacial areas

$\mu$ ( $\mu m$ )	$\sigma$ ( $\mu m$ )	$a_{CO_2}/a_{geo}$	$a_{O_2}/a_{geo}$	$a_{O_2}/a_{CO_2}$
84	121	0.32	0.75	2.35
358	250	0.54	0.94	1.75

tion that was measured using ultra sound (log-normal,  $\mu = 84 \mu m$ ,  $\sigma = 121 \mu m$ , with a minimum bubble size of  $10 \mu m$ ) and a good log-normal fit of the distribution obtained by Machon et al. (1997) in a non-coalescing electrolyte system ( $\mu = 358 \mu m$ ,  $\sigma = 250 \mu m$ ). The results are shown in Table 6. These results only indicate that the measured lower mass transfer coefficient for  $CO_2$  in comparison  $O_2$  is likely to be due to the depletion of small bubbles. The results in the last row of Table 6 are in good agreement with a results that were obtained using a similar analysis using the work of Midoux et al. (1980). The extent of this effect is quite dependent on the size distribution and on the model assumptions.

From the observed phenomena, it can be concluded that the most likely explanation for the obtained lower mass trans-

fer coefficient with carbon dioxide is the high gas phase conversion, which causes almost complete depletion of small bubbles and therefore lowers the effective interfacial area.

#### 4. Conclusions

In the present study, design rules for continuous physical mass transfer experiments are derived, to obtain the highest accuracy for the determination of the volumetric mass transfer coefficient. It was shown that concentration measurement in the liquid phase is favourable when  $m\Phi_L < \Phi_G$ . In other cases measurement in the gas phase is favourable (assuming the same experimental accuracy). Furthermore, in case of liquid phase concentration measurement desorption is more accurate and in case of gas phase measurement absorption is the preferred direction of mass transfer.

Desorption of oxygen from a carbonate/bicarbonate buffer solution was used to study the effect of the catalyst addition, for the construction of the Danckwerts-plot, on the hydrodynamics of the system. It was confirmed by comparing absorption and desorption rates in water that these two processes are identical, but in a different direction. It was shown that the addition of the catalyst (up to 0.2M sodium hypochlorite) did not affect the desorption rate of oxygen. The effect of catalyst addition on the hydrodynamics of the system is therefore negligible.

The volumetric mass transfer coefficient of oxygen was, however, much larger (64%) compared to the  $k_L a$  of carbon dioxide. This is most likely caused by the higher solubility of carbon dioxide compared to oxygen, which causes a higher gas phase conversion. In case of a broad size distribution containing a relatively large fraction of small ( $< 100 \mu m$ ) bubbles, these small bubbles are at an earlier stage (almost) completely depleted, when they contain carbon dioxide compared to when they contain oxygen. This can cause a lower effective interfacial area with  $CO_2$ . Mass transfer experiments with a low gas phase conversion (here: with oxygen), are therefore preferred, as the measured mass transfer parameters are less affected by the gas phase RTD and the shape of the bubble size distribution.

## Notation

$a$	interfacial area, $\text{m}^2/\text{m}^3$
$c_A$	concentration of component A, $\text{mol}/\text{m}^3$
$d_{32}$	Sauter mean bubble diameter, m
$D$	impeller diameter, m
$D_A$	diffusion coefficient of component A, $\text{m}^2/\text{s}$
$g$	gravitational constant, $\text{m}/\text{s}^2$
$k_{1,\text{app}}$	apparent (pseudo)-first-order reaction rate constant, $\text{s}^{-1}$
$k_c$	forward reaction rate constant of the catalyzed reaction of $\text{CO}_2$ with water, $\text{m}^3/(\text{mol s})$
$k_{\text{H}_2\text{O}}$	forward reaction rate constant of the reaction of $\text{CO}_2$ with water, $\text{s}^{-1}$
$k_{\text{OH}^-}$	forward reaction rate constant of the reaction of $\text{CO}_2$ with hydroxyl ions, $\text{m}^3/(\text{mol s})$
$k_L$	liquid phase mass transfer coefficient, $\text{m}/\text{s}$
$m$	ratio of solubility in the liquid phase and in the gas phase, dimensionless
$N$	stirring speed, rps
$N_P$	power number, dimensionless
$P, P_g$	(gassed) power input, W
$R_A$	absorption rate, $\text{mol}/\text{s}$
$u_G$	superficial gas velocity, $\text{m}/\text{s}$
$V_L$	liquid volume, $\text{m}^3$
$W$	impeller blade width, m

## Greek letters

$\varepsilon$	gas fraction, dimensionless
$\mu$	mean in a log-normal distribution, m
$\rho$	liquid density, $\text{kg}/\text{m}^3$
$\sigma$	variance in a log-normal distribution, m
$\varphi_G$	space velocity of the gas, $\Phi_G/V_L$ , $\text{s}^{-1}$
$\Phi$	flow rate, $\text{m}^3/\text{s}$

## Subscripts

0	inlet
geo	geometric
G	gas phase
L	liquid phase

## Acknowledgements

The authors wish to gratefully acknowledge E. van Brandenburg for her contribution to the experimental work and B. Knaken for the construction of the experimental set-up and the technical support.

## References

- Alper, E., Deckwer, W.-D., Danckwerts, P.V., 1980. Comparison of effective interfacial areas with the actual contact area for gas absorption in a stirred cell. *Chemical Engineering Science* 35, 1263–1268.
- Benadda, B., Prost, M., Ismaili, S., Bressat, R., Otterbein, M., 1994. Validation of the gas-lift capillary bubble column as a simulation device

- for a reactor by the study of  $\text{CO}_2$  absorption in  $\text{Na}_2\text{CO}_3/\text{NaHCO}_3$  solutions. *Chemical Engineering and Processing* 33, 55–59.
- Carberry, J.J., Varma, A., 1987. *Chemical Reaction and Reactor Engineering*. Marcel Dekker, New York.
- Cents, A.H.G., 2003. Mass transfer and hydrodynamics in stirred gas–liquid–liquid contactors. Ph.D. Thesis, University of Twente, The Netherlands.
- Cents, A.H.G., Brilman, D.W.F., Versteeg, G.F., 2001. Gas absorption in an agitated gas–liquid–liquid system. *Chemical Engineering Science* 56, 1075–1083.
- Cents, A.H.G., Kersten, S.R.A., Brilman, D.W.F., 2003. Gas-phase RTD measurement in gas and gas–solids reactors using ultrasound. *Industrial and Engineering Chemistry Research* 42, 5506–5515.
- Cents, A.H.G., Brilman, D.W.F., Versteeg, G.F., Wijnstra, P.J., Regtien, P.P.L., 2004. Measuring bubble, drop and particle sizes in multiphase systems with ultrasound. *A.I.Ch.E. Journal* 50, 2750–2762.
- Cents, A.H.G., Brilman, D.W.F., Versteeg, G.F., in press.  $\text{CO}_2$  absorption in carbonate/bicarbonate solutions: the Danckwerts criterion revisited. *Chemical Engineering Science*.
- Danckwerts, P.V., 1950. Absorption by simultaneous diffusion and chemical reaction. *Transactions of the Faraday Society* 46, 300–304.
- Danckwerts, P.V., Sharma, M.M., 1966. Absorption of carbon dioxide into solutions of alkalis and amines. *The Chemical Engineer CE* 244–280.
- Danckwerts, P.V., Kennedy, A.M., Roberts, D., 1963. Kinetics of  $\text{CO}_2$  absorption in alkaline solutions—II absorption in a packed column and tests of surface renewal models. *Chemical Engineering Science* 18, 63–72.
- Díaz, M., Vega, A., Coca, J., 1987. Correlation for the estimation of gas–liquid diffusivity. *Chemical Engineering Communications* 52, 271–281.
- Hallensleben, J., 1980. Simultaner Stoffaustausch von  $\text{CO}_2$  und Sauerstoff an Einzelblasen und in Blasenschwärmen. Ph.D. Thesis, Universität Hannover.
- Hughmark, G.A., 1980. Power requirements and interfacial area in gas–liquid turbine agitated systems. *Industrial and Engineering Chemistry; Process Design and Development* 19, 638–641.
- Kon, N.S., Sandall, O.C., 1978. Comparison of effective interfacial areas with the actual contact area for gas absorption in an agitated vessel. *Canadian Journal of Chemical Engineering* 56, 658–689.
- Linek, V., Vacek, V., Beneš, P., 1987. A critical review and experimental verification of the correct use of the dynamic method for the determination of oxygen transfer in aerated agitated vessels to water, electrolyte solutions and viscous liquids. *Chemical Engineering Journal* 34, 11–34.
- Lorimer, J.W. (Ed.), 1979. *IUPAC Solubility Data Series*. vols. 5/6 and 43. Pergamon Press, Oxford.
- Machon, V., Pácek, A.W., Nienow, A.W., 1997. Bubble sizes in electrolyte and alcohol solutions in a turbulent stirred vessel. *Transactions of the Institution of Chemical Engineers* 75, 339–348.
- Mehta, V.D., Sharma, M.M., 1971. Mass transfer in mechanically agitated gas–liquid contactors. *Chemical Engineering Science* 26, 461–479.
- Midoux, N., Laurent, A., Charpentier, J.C., 1980. Limits of the chemical method for the determination of physical mass transfer parameters in mechanically agitated gas–liquid contactors. *A.I.Ch.E. Journal* 26, 157–162.
- Richards, G.M., Ratcliff, G.A., Danckwerts, P.V., 1964. Kinetics of  $\text{CO}_2$  absorption—III first order reaction in a packed column. *Chemical Engineering Science* 19, 325–328.
- Schlüter, V., Deckwer, W.-D., 1992. Gas–liquid mass transfer in stirred vessels. *Chemical Engineering Science* 47, 2357–2362.
- Schumpe, A., Deckwer, W.-D., 1980. Analysis of chemical methods for determination of interfacial areas in gas–liquid dispersions with non-uniform bubble sizes. *Chemical Engineering Science* 35, 2221.
- Weisenberger, S., Schumpe, A., 1996. Estimation of gas solubilities in salt solutions at temperatures from 273 K to 363 K. *A.I.Ch.E. Journal* 42, 298–300.